

# Fabrication of Flexible Microlens Array through Vapor-induced Room Temperature Dewetting on Plasma Treated Parylene-C

Xiaopeng Bi, Wen Li, *IEEE Member*

**Abstract**— Microlens arrays have been widely used as an essential component in many optical systems. The conventional fabrication techniques, such as ink-jet printing, photoresist thermal reflow, grayscale photolithography, and LIGA process have some drawbacks in aspects of process complexity and high fabrication cost. This paper presents a low-temperature, rapid and cost-effective method to successfully generate SU-8 microlens arrays on biocompatible Parylene-C surfaces. Vapor-induced SU-8 dewetting has been achieved on chemically modified Parylene-C surfaces that were selectively pre-treated with O<sub>2</sub> or SF<sub>6</sub> plasma. By this technique, the SU-8 droplets are self-organized onto desired positions to form a microlens array. This method is also suitable for production of microlens array on curved surfaces. The progress of dewetting has been studied by both experiment and simulation.

## I. INTRODUCTION

Microlens arrays have been widely used as an essential component in many optical systems, including digital display, integral imaging, high-density data storage and optical communications [1-4]. In particular, due to the capability of improvement of light out-coupling efficiency, the integration of microlens array with micro-light-emitting diodes ( $\mu$ -LEDs) has become a promising solution as the light source in applications that require high-resolution multisite illumination, for example, the fast growing field of optical neural stimulations [5].

A variety of strategies have been previously reported for fabricating microlens arrays, such as ink-jet printing [6], photoresist thermal reflow [7], grayscale photolithography [8], and LIGA process [9]. While these approaches have demonstrated the ability to produce microlens arrays, most of them also have some drawbacks. For example, the ink-jet printing method, frequently operated in drop-on-demand (DOD) mode, is a highly automated process with which patterns of convex microlenses can be written directly onto a substrate by dispensing droplets of optical material at target positions. However, lens size and alignment inaccuracy is the limitation for ink-jet printing. Photoresist thermal reflow is another commonly used approach to generate microlens arrays. The photoresist micro-structures are first created by the conventional photolithography and subsequently baked over its glass transition temperature. Micro-printing or

reactive ion etching is often required for lens replication to transfer the photoresist microlens profile into other materials with appropriate optical properties. Besides the high processing temperature, the complexity of involved fabrication is also a concern. The grayscale photolithography technology employs a unique mask with a transmission gradient to directly create a 3-D micro-pattern on the photoresist with designed profile of lens array, but the complication and high cost in making grayscale photomasks is a main problem.

In this paper, we present a low-temperature, rapid and cost-effective method for the fabrication of microlens arrays. Vapor-induced dewetting process has been applied on chemically modified surfaces that were selectively pre-treated with low-energy O<sub>2</sub> and SF<sub>6</sub> plasma. SU-8 microlens arrays have been successfully achieved on the Parylene-C substrate, which is commonly used as the polymeric coating material in biomedical micro- and nano- devices due to its flexibility, biocompatibility and optical transparency [10]. Although significant efforts have been devoted to studying the mechanisms and dynamics of dewetting [11, 12], there have been few dewetting experiments on chemically patterned surfaces with non-uniform wettability. Compared to the uncontrolled dewetting, our employment of the plasma pre-treatment enables the self-organization of SU-8 droplets to form an array directly on desired positions during dewetting. In addition, the feasibility of dewetting at room temperature benefits the integration of materials and components that cannot stand a high temperature. Such a process is also suitable for mass production of microlens arrays on curved polymeric surfaces, which potentially has broad applications in optical and biomedical fields.

## II. METHODS AND FABRICATION

### A. Plasma Pre-treatments

In principle, the dynamic change of low-viscosity SU-8 resist in a dewetting process is driven by the capillary force as a consequence of surface energy minimization of films, substrates and interfaces. Therefore, an important parameter in the controlled dewetting process is the liquid contact angle (CA) with respect to the target location of a substrate, which has been seriously taken into consideration. First, the liquid coating with a high equilibrium CA is desired due to its strong tendency to rupture on the substrate and trigger the dewetting process. Second, the microlens array is expected to form spontaneously on pre-defined positions, which requires a large decrease in the CA on those target spots.

Based on our previous study, low-energy plasma treatment offers a facial route to tune the surface wettability [13, 14]. It



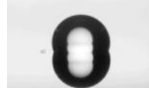


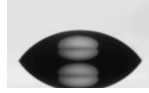
Research supported by NSF CAREER ECCS-1055269.

X. Bi is with the Department of Electrical and Computer Engineering, Michigan State University, East Lansing, MI 48824 USA (phone: 517-355-3299; fax: 517-353-1980; e-mail: bixiao@msu.edu).

W. Li is with the Department of Electrical and Computer Engineering, Michigan State University, East Lansing, MI 48824 USA (e-mail: wenli@egr.msu.edu).

can modify only the superficial molecular layers of the material without affecting the bulk property. The oxygen ( $O_2$ ) and sulfur hexafluoride ( $SF_6$ ) plasma treatments have been found to be effective in altering the surface wettability to hydrophilicity and hydrophobicity, respectively. This can be attributed to the variation of surface roughness and plasma-induced surface chemistry [14]. The CAs of both deionized water and SU-8 2000.2 on plasma-treated and untreated Parylene-C films have been measured to characterize the surface wettability, using a contact angle analysis system. For these studies, the plasma was applied at a fixed radio-frequency (RF) power of 100 W for 1 min with each gas.

TABLE I. CONTACT ANGLES ON PARYLENE-C

Liquid	Parylene-C		
	Untreated	$O_2$ plasma treated	$SF_6$ plasma treated
Water	85.2° 	27.5° 	112.7° 
SU-8 2000.2	~0° 	~0° 	53.6° 

As shown in Table I, the complete wetting of SU-8 (CA ~ 0°) was observed on untreated Parylene-C, and also hydrophilic Parylene-C treated by  $O_2$  plasma. On the other hand, SU-8 exhibits a CA of 53.6° on the  $SF_6$  plasma-treated Parylene-C. The CAs of the SU-8 droplets are lower than those of the water droplets on the same surface, mainly due to the high viscosity of SU-8. More importantly, different plasma treatments resulted in significant changes in the SU-8 CAs, and thus are suitable to be applied in the proposed controlled dewetting experiments, as described in the following section.

### B. Fabrication

To achieve the controlled SU-8 dewetting on a Parylene substrate, we treated the whole Parylene-C surface by  $SF_6$  plasma, except the desired areas of microlens array, which was treated by  $O_2$  plasma. The fabrication process is illustrated in Fig. 1. In short, 5 $\mu$ m-thick Parylene-C films were prepared through vacuum chemical vapor deposition (CVD) on two-inch silicon wafers.  $SF_6$  plasma was then applied to treat the entire Parylene-C surface for 1 min with a flow rate of 20 sccm and a RF power of 100 W, using a plasma etcher. Photoresist S1813 was spin-coated for 40 s, followed by baking at 110 °C on the hot plate for 1 min. The photoresist was used to pattern the openings on the surface for the targeted spots of microlenses through conventional photolithography. For the proof-of-concept, we designed a square array of circular patterns with the diameter of 100  $\mu$ m and the separation of 150  $\mu$ m. After the UV exposure for 15 s and the following development in Developer 352,  $O_2$  plasma treatment was carried out for 1 min with a flow rate of 15 sccm

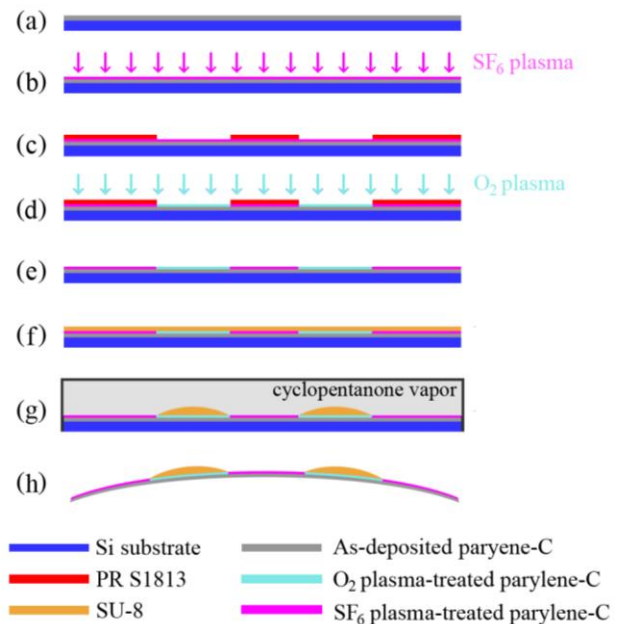


Figure 1. Fabrication process of vapor-induced dewetting.

and a RF power of 100 W, in order to switch the wettability of the opening areas (the target positions of microlenses) from hydrophobicity to hydrophilicity. After the remained photoresist was removed by acetone, an ultrathin layer of SU-8 2000.2 was spin-coated on the plasma modified Parylene-C surface for 40 s and an approximate thickness of 200 nm was obtained. Subsequently, the sample was placed into the vapor atmosphere of cyclopentanone, a solvent of SU-8 resin, in order to reduce the resist viscosity for the dewetting step. The course of dewetting was recorded by a camera through a stereomicroscope. After the completion of SU-8 dewetting, the sample was soaked in the deionized water to release the Parylene-C film off the silicon substrate to achieve a flexible microlens array.

## III. RESULTS

### A. Surface Morphology

Fig. 2 shows the evolution of surface morphology of a 7 × 7 array during the process of the vapor-induced SU-8 dewetting. At the beginning, the coating of SU-8 thin films failed to remain continuous at certain spots where defects existed, such as scratches and tiny dusts. Dry holes gradually formed on these locations and started to extend. During the growth of these dry holes, the rims of the liquid-solid contact lines developed along outward directions except in contact with the microlens areas where had been treated by  $O_2$  plasma. Break-ups often occurred on the rims near the lens spots as the adjacent contact lines departed those spots and kept driving the movement of liquid material. After the break-ups, isolated droplets formed on the  $O_2$ -plasma-treated positions. From the observation, the dewetting completed at room temperature in 50 min. This dewetting speed could be increased by increasing the temperature of the vapor of SU-8 solvent. A microscopy image of the final pattern of a 6 × 10 microlens array after the dewetting process is shown in Fig. 3.

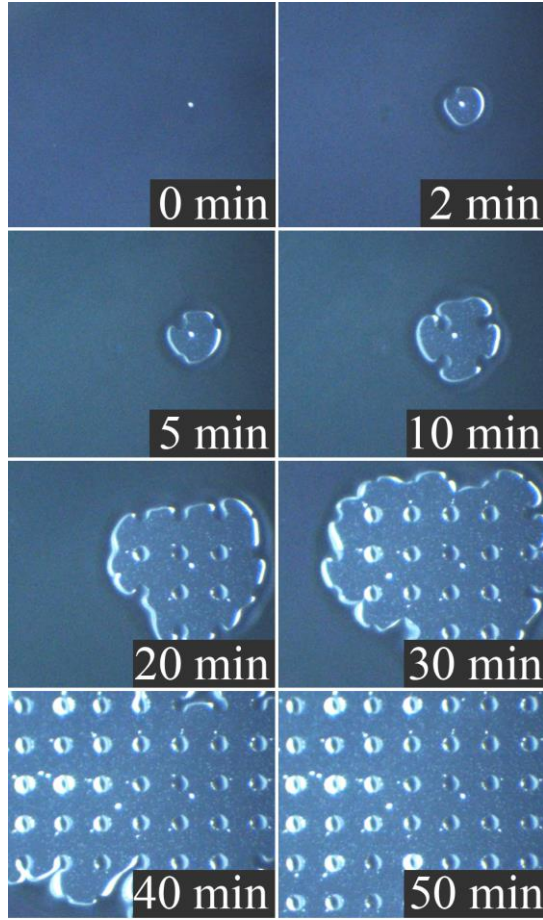


Figure 2. Evolution of surface morphology of a  $7 \times 7$  array during the process of the vapor-induced SU-8 dewetting.

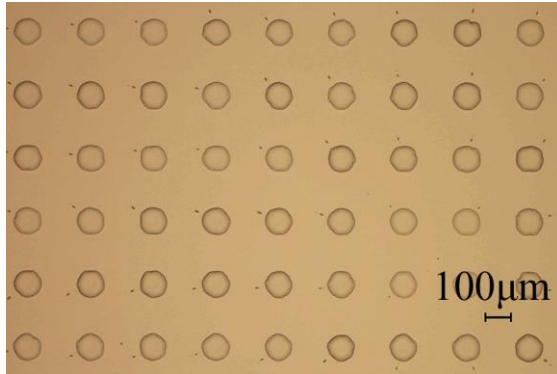


Figure 3. Microscopy image of the final pattern of a  $6 \times 10$  microlens array fabricated by the vapor-induced room temperature dewetting.

### B. Uniformity

The profile of the microlens array has been characterized by a profilometer, as shown in Fig. 4, in order to study the uniformity of microlenses over the entire array. In average, the height of the microlenses is  $1.59 \pm 0.20 \mu\text{m}$ . The corresponding average CA is  $3.6 \pm 0.5^\circ$ .

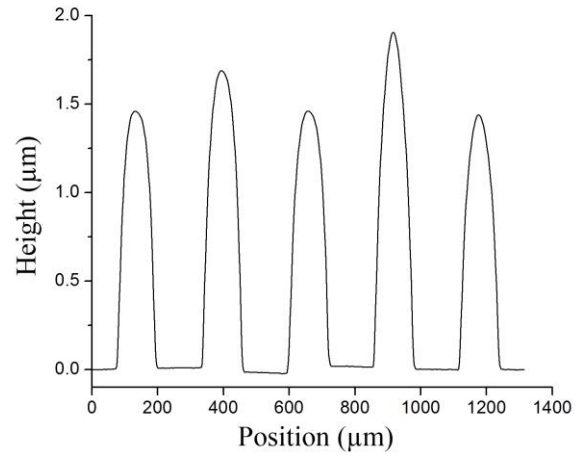


Figure 4. The profile of microlenses fabricated by the vapor-induced room temperature dewetting.

## IV. SIMULATION

We further studied the SU-8 dewetting process using a computational model. The thickness profile of the SU-8 coating layer is represented by the function  $h(x, y, t)$ . Because the dewetting process was carried out in the saturated vapor environment of cyclopentanone, it is assumed that there is no evaporation of the solvent from the SU-8 coating. Therefore, the equation expressing conservation of mass is given as:

$$h_t = -\nabla \cdot Q, \quad (1)$$

where  $Q$  denotes the flux rate. Applying the slow-flow and small-slope approximations in Navier-Stokes equations, as well as the no-slip boundary condition at the substrate,  $Q$  is proportional to the pressure gradient:

$$Q = -\frac{h^3}{3\mu} \nabla p. \quad (2)$$

The pressure  $p$  includes capillary and disjoining contributions:

$$p = -\sigma \nabla^2 h - \Pi, \quad (3)$$

$$\Pi = \frac{(n-1)(m-1)}{h_0(n-m)} \sigma (1 - \cos\theta) \left[ \left(\frac{h_0}{h}\right)^n - \left(\frac{h_0}{h}\right)^m \right], \quad (4)$$

where  $\sigma$  is the surface tension and  $\Pi$  is the disjoining pressure [12], which is governed by a long-range attractive potential and a short-range repulsive potential, in order to stabilize the calculation as the coating thickness approaches zero. The characteristic thickness  $h_0$  is small compared to the average thickness of the coating layer and typically on the order of a few nanometers. In this study, the values  $(n, m, h_0) = (3, 2, 50 \text{ nm})$  was used. The position dependence of contact angle  $\theta$  represents the chemical patterning on the surface. By combining (1) to (4), the final form of the evolution equation can be expressed as:

$$h_t = -\frac{\sigma}{3\mu} \nabla \cdot \left[ h^3 \nabla \left( \nabla^2 h + \frac{(n-1)(m-1)}{h_0(n-m)} \sigma (1 - \cos\theta) \left[ \left(\frac{h_0}{h}\right)^n - \left(\frac{h_0}{h}\right)^m \right] \right) \right], \quad (5)$$

This equation was numerically solved by applying the alternating direction implicit (ADI) scheme [15] and the Newton's method (second-order Crank-Nicolson scheme). The adaptive time-stepping procedure was employed to increase the computational efficiency. A 1-D simulation result is presented in Fig. 5. By setting up CAs on different regions, which are resulted from the O<sub>2</sub> or SF<sub>6</sub> plasma pre-treatment, the final profile presents a similar morphology as the experimental result. The thickness of the coating layer approaches zero on surfaces treated by SF<sub>6</sub> plasma, while the ordered isolated droplets form spontaneously at the lens spots treated by O<sub>2</sub> plasma. The evolution equation is proved to be effective to calculate and predict the dewetting process.

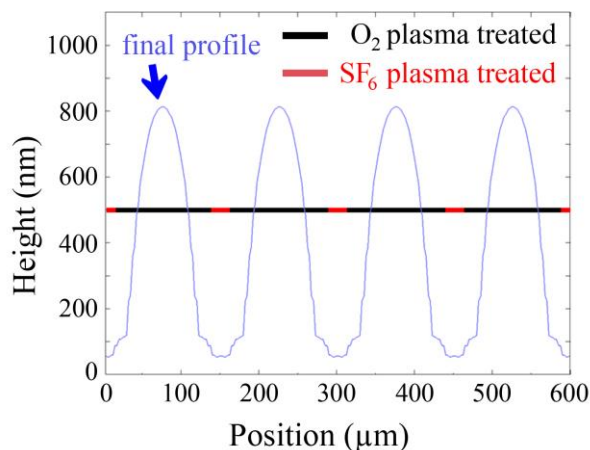


Figure 5. The simulation result of dewetting process by numerically solving the evolution equation for the coating thickness.

## V. CONCLUSIONS

We have demonstrated a rapid and cost-effective method in which the vapor-induced dewetting was applied to achieve flexible SU-8 microlens arrays on the Parylene-C substrates at room temperature. Its intergration with  $\mu$ -LEDs provides a possible solution as the light source to achieve high-resolution multisite illumination, which is in demand in many optical and biomedical applications such as optogenetics.

## REFERENCES

- [1] M. Martinez-Corral, B. Javidi, R. Martinez-Cuenca, and G. Saavedra, "Integral imaging with improved depth of field by use of amplitude-modulated microlens arrays," *Appl. Optics*, vol. 43, Nov. 2004, pp. 5806–5813.
- [2] J. Arai, H. Kawai, and F. Okano, "Microlens arrays for integral imaging system," *Appl. Optics*, vol. 45, Dec. 2006, pp. 9066–9078.
- [3] K. S. Hong, J. Wang, A. Sharonov, D. Chandra, J. Aizenberg, and S. Yang, "Tunable microfluidic optical devices with an integrated microlens array," *J. Micromech. Microeng.*, vol. 16, Aug. 2006, pp. 1660–1666.
- [4] L. P. Zhao, N. Bai, X. Li, L. S. Ong, Z. P. Fang, and A. K. Asundi, "Efficient implementation of a spatial light modulator as a diffractive optical microlens array in a digital Shack–Hartmann wavefront sensor," *Appl. Optics*, vol. 45, Jan. 2006, pp. 90–94.

- [5] N. Grossman, V. Poher, M. S. Grubb, G. T. Kennedy, K. Nikolic, B. McGovern, et al., "Multi-site optical excitation using ChR2 and micro-LED array," *J. Neural Eng.*, vol. 7, Feb. 2010, 016044.
- [6] J. Y. Kim, N. B. Brauer, V. Fakhfour, D. L. Boiko, E. Charbon, G. Grutzner, et al., "Hybrid polymer microlens arrays with high numerical apertures fabricated using simple ink-jet printing technique," *Opt. Mater. Express*, vol. 1, Jun. 2011, pp. 259–269.
- [7] E. Roy, B. Voisin, J. F. Gravel, R. Peytavi, D. Boudreau, and T. Veres, "Microlens array fabrication by enhanced thermal reflow process: Towards efficient collection of fluorescence light from microarrays," *Microelectron. Eng.*, vol. 86, Nov. 2009, pp. 2255–2261.
- [8] K. Totsu, K. Fujishiro, S. Tanaka, and M. Esashi, "Fabrication of three-dimensional microstructure using maskless gray-scale lithography," *Sensor. Actuat. A-Phys.*, vol. 130, Aug. 2006, pp. 387–392.
- [9] D. S. Kim, H. S. Lee, B. K. Lee, S. S. Yang, T. H. Kwon, and S. S. Lee, "Replications and analysis of microlens array fabricated by a modified LIGA process," *Polym. Eng. Sci.*, vol. 46, Apr. 2006, pp. 416–425.
- [10] W. Li, D. C. Rodger, E. Meng, J. D. Weiland, M. S. Humayun, and Y. C. Tai, "Flexible parylene packaged intraocular coil for retinal prostheses," in *Proc. Int. Conf. MMB*, Okinawa, Japan, May 2006, pp. 105–108.
- [11] C. V. Thompson, "Solid-state dewetting of thin films," *Annu. Rev. Mater. Res.*, vol. 42, 2012, pp. 399–434.
- [12] L. W. Schwartz, R. V. Roy, R. R. Eley, and S. Petrash, "Dewetting patterns in a drying liquid film," *J. Colloid Interf. Sci.*, vol. 234, Feb. 2001, pp. 363–374.
- [13] X. Bi, N. L. Ward, B. P. Crum, and W. Li, "Plasma-treated switchable wettability of parylene-C surface," in *Proc. 7th Int. Conf. NEMS*, Kyoto, Japan, Mar. 2012, pp. 222–225.
- [14] X. Bi, B. P. Crum, and W. Li, "Super hydrophobic Parylene-C produced by consecutive O<sub>2</sub> and SF<sub>6</sub> plasma treatment," *J. Microelectromech. S.*, to be published.
- [15] T. P. Witelski and M. Bowen, "ADI schemes for higher-order nonlinear diffusion equations," *Appl. Numer. Math.*, vol. 45, May 2003, pp. 331–351.